title*Ab Initio* studies of the atomic structure and electronic density of states of pure and hydrogenated *a*-Si

Ariel A. Valladares* and Fernando Alvarez

Instituto de Investigaciones en Materiales, UNAM, Apartado Postal 70-360, México, D. F., 04510, MEXICO

Zhihua Liu

Molecular Simulations, Inc., 9685 Scranton Road, San Diego, CA, 92121, USA

Juergen Stitcht

SciCo Inc., 5031 Palermo Dr., Oceanside, CA, 92057, USA

John Harris

Institut fuer Festkoeperforschung, Forschungszentrum, Juelich GmbH, D-52425, Juelich, Germany

(October 24, 2018)

We propose a method to simulate *a*-Si and *a*-Si:H using an *ab initio* approach based on the Harris functional and thermally amorphisized periodically continued cells with at least 64 atoms, and calculate their radial distribution functions. Hydrogen incorporation was achieved via diffusive random addition. The electronic density of states (DOS) is obtained using density functional theory with the aid of both the Harris-functional and Kohn-Sham-LDA approaches. Two time steps are used, 2.44 and 10 fs for the pure, and 0.46 and 2 fs for the hydrogenated, to see their effect on the topological and DOS structure of the samples. The calculated long time-step radial features of *a*-Si are in very good agreement with experiment whereas for *a*-Si:H the short time-step partial and total radial features agree well; for the long time-step simulation molecular hydrogen appears during annealing. The long time-step *a*-Si has a well defined gap with two dangling bonds, that clears and increases upon hydrogen addition and relaxation, as expected. The short time-step structures have more defects, both dangling and floating bonds, that are less characteristic of a good sample; however the radial structures of *a*-Si:H are in better agreement with experiment indicating that the experimental work was done on defective samples.

(PACS: 71.23.Cq, 71.15.Pd, 71.55.Jv, 73.61.Jc)

I. INTRODUCTION

The scientific and technological relevance of *a*-Si, pure and hydrogenated, is well known and needs not be emphasized here; early work on the atomic structure of the pure amorphous material started more than four decades ago, both

experimentally and theoretically. Experimentally, work on the amorphous phases of pure germanium and silicon evolved in parallel, beginning with the electrolytic approach of Szekely[1] in 1951 and the pioneering efforts of Richter and Breitling[2] in 1958. Theoretically, the first atomic models of both *a*-Si and *a*-Ge appeared in the literature over thirty years ago. Grigorovici and Manaila[3] and Coleman and Thomas[4] in 1968 suggested structures based on arrangements of closely packed simplified Voronoi polyhedra that have the shape of truncated tetrahedra both eclipsed and staggered 60° about their common bond, leading to rings of five atoms and to boatlike rings of six atoms, as in the carbon and silicon amorphous clusters that we have recently studied.[5] As is well known, fivefold symmetry is non-crystallographic and therefore yields an amorphouslike diffraction pattern with broad maxima. The eclipsed configuration with a fivefold symmetry structure is energetically unfavorable in the crystalline phases but occurs in the amorphous form since atomic arrangements with a large internal energy can appear in such frozen structures.[6]

It was soon realized that such pure structures were incapable of being doped with donors or acceptors, due to the presence of dangling bonds that masked the existence of an energy gap in the density of states (DOS) spectrum, and the search began to find a solution to this problem. Spear and Lecomber[7] discovered that if amorphous silicon is grown in the presence of hydrogen the naturally existing dangling bonds passivate revealing, in this manner, the presence of the gap. It was then possible to introduce dopants whose influence was clearly seen. This radically transformed the study of amorphous semiconductors from an academic subject to a technologically relevant one that has led to the design of devices that are presently used in many applications. In this manner the study of hydrogenated amorphous silicon flourished[8] and became one of the most important subjects in the area of amorphous semiconductors.

All these materials have been experimentally produced and characterized without theoretical guidelines that atomistic simulations may provide. In particular, several experimental radial distribution functions (RDFs) have been obtained for pure amorphous silicon, and some for hydrogenated amorphous silicon, using a variety of techniques from X-ray to neutron diffraction, in order to better comprehend their atomic structure. A consistent picture has emerged for the structure of *a*-Si. However, for *a*-Si:H the neutron diffraction experiments needed to probe the hydrogen presence are relatively more recent[9] and the information is scarce; nevertheless some interesting structural features have been identified for this system, which makes it particularly appealing for theoretical simulations.

It is clear that, in principle, a full theoretical description of the properties of an amorphous solid depends on a complete knowledge of the atomic structure. However, for these solids there are an infinite number of possible structures and the best we can do in order to characterize their atomic arrangement is to use the RDF, also known as pair distribution function. Defined as $4\pi r^2 \rho(r) dr$, where $\rho(r)$ is the density of particles at point r, the RDF

gives the average number of pairs of atoms separated by a distance lying between r and $r + dr$. A given structure generates a well defined RDF but a given RDF corresponds to many atomic structures; that is, there is not a one to one correspondence between a given structure and its corresponding RDF. For this reason, clusters with a particular local structure have been used to simulate the amorphous bulk and this has shed light on the effect of specific atomic arrangements on the electronic properties of these materials.[5]

The experimental work of Refs. 10 to 16 for *a*-Si and Refs. 17 and 18 for *a*-Si:H will be considered in this paper. For hydrogenated silicon, Ref. 18 reports the only complete study of the total RDF, together with the partials for Si-Si, Si-H and H-H.

On the theoretical side, a considerable amount of work has been done to simulate the atomic structure of *a*-Si, while the atomic structure of *a*-Si:H has been the subject of more recent work. A knowledge of their atomic topology leads to better and more realistic calculations of the electronic structure of these systems. These efforts can be classified via two extreme types: i) calculations that are carried out in samples that are constructed essentially "to order" by switching bonds and adjusting dihedral angles, and that use *ad hoc* classical, parameter-dependent potentials constructed for the specific purpose of describing them; ii) quantum methods, parameterized and *ab initio*, that can deal from the outset with the thermalization processes that generate the amorphous structure, and the study of their corresponding electronic properties. In between, one finds a variety of hybrid approaches. In the present work we shall not consider the beautiful, computationally cost-effective, work that has been done with classical techniques in very large supercells of *a*-Si that contain tens of thousands atoms (see for instance Ref. 19 and work cited therein), since such methods are not transferable to other amorphous materials. Moreover, it is necessary to generate new *ad hoc* parameters and potentials in order to deal with new materials, either from experimental results or from *ab initio* calculations. Furthermore, it has been established[20] that even though some of these potentials describe the RDF, they fail in differing degrees to describe other properties of the amorphous lattice, and this is understandable since no matter how good a classical approach may simulate the atomic interactions, there will be quantum properties beyond the capability of these techniques.

Quantum methods answered some of the unsolved questions left by the classical approaches, and were themselves of several kinds. For example, there has been some interesting work done using tight binding methods for pure silicon,[21] where a transferable model is found by fitting the energies of silicon in various bulk crystal structures and examining functional parameterizations of the tight binding forms. For hydrogenated silicon a transferable model has also been found by fitting it to silane.[22] On the other hand, there are *ab initio* methods that attempt to answer all the

questions from first principles and are generally applicable without adjustment of parameters, but are very demanding in computer resources and so are limited to handling relatively small amorphous cells. The question is, how generally can an *ab initio* method that uses a reasonably sized supercell be applied, and how accurate can one expect the results to be? The present work addresses these issues for amorphous silicon and for hydrogenated amorphous silicon.

II. ANTECEDENTS

For our purposes, the theoretical calculations described in Car and Parrinello[23] through to Lee and Chang[28] for *a*-Si and in Buda *et al.*[29] through to Tuttle and Adams[31] for *a*- Si:H are appropiate since they approach the structural problem by generating amorphous cells using first-principles quantum methods.

More than a decade ago Car and Parrinello[23] performed the first *ab initio* molecular dynamics (MD) study in an fcc cell with 54 atoms of silicon using their plane wave MD method. In their approach a non-local pseudopotential was used together with the parameterized local density (LDA) form of Perdew and Zunger for the exchange-correlation effects. They obtained good agreement with the experimental RDF of *a*-Ge, rescaled to simulate *a*-Si, up to the second radial peak and argued that because of the size of the cell used distances larger that 6 Å could not be studied. They pointed out that the comparison of the simulated atomic structure to the experimental ones should be done with care since a large number of defects were found in their results. The simulation was started above the melting point, at about 2,200 K, and then the liquid was allowed to evolve for $\approx 0.7 \times 10^{-12}$s before it was quenched down to $\approx$ 300 K at a cooling rate of $\approx 2 \times 10^{15}$ K/s. During the initial quenching the volume of the cell was gradually increased to 1080 Å^3, the crystalline value. This technique of quenching from the melt has been used in subsequent work although handling the transition from the liquid to the amorphous phase is not an easy task since a volume change has to be dealt with and because liquid silicon is metallic with an average coordination number of between 6 and 7, the quenching preserves some of this overcoordination.

For example, Drabold *et al.*[24] use a density functional theory, local density approximation (DFT-LDA), molecular dynamics approach developed by Sankey *et al.*[32] based on a simplification of the Kohn-Sham equations as developed by Harris,[33] and starting with a 64-atom simple cubic cell in the diamond structure with one vacancy, they generate an "incompletely melted" sample by heating it up to 8,000 K. The free evolution of the cell then results in the system acquiring a highly disordered liquidlike structure before final quenching to a solid. They state that their results for the RDF agree well with experiment, without making a detailed, direct comparison. They find only four coordination defects, two dangling and two floating bonds, for appropiate values of the rate of free evolution of the cell. After

annealing at 300 K only two defects survived.

A more complete report of the Car and Parrinello results is given in Stich *et al.*,[25] where a cooling rate from the melt of 10^{14} K/s is used. This slower cooling rate seems to be sufficient to recover a tetrahedral network that nevertheless contains several coordination defects as well as a large fraction of distorted bonds. Annealing at 900 K reduces the defects and the RDF they obtain has two peaks that seem to agree with the first two peaks of experiments. The study performed by Drabold *et al.* was extended[26] to the 216 atom periodic supercell of Wooten, Winer and Weaire[27] and a more complete analysis of the relationship of structural defects, spectral defects and interatomic distances was carried out. Lee and Chang[28] perform *ab initio* simulations on a 64-atom silicon cell and quench incompletely melted samples as in Ref. 24, but they find that the third peak of the RDF practically disappears, and that more dangling and floating bonds occured than in previously generated samples from liquid-quenched simulations, and than in the samples generated by Drabold *et al.*[24]

Theoretical work on *a*-Si:H has been less abundant because the experimental RDF results are limited and it is more difficult to model interactions of H and Si and cope with the time steps needed for computer simulations of hydrogen diffusion. In addition, the strong dependence of the *a*-Si:H structure on deposition conditions has to be reflected in the simulations, together with the chemical reactivity of hydrogen and its zero point energy; all this requires the use of quantum mechanical methods. The *ab initio* work performed for this system is found in Refs. 29 to 31. In some of the models H is incorporated into a previously created amorphous network of pure *a*-Si by hand,[30] with the consequent inhibition of hydrogen diffusion, whereas Buda *et al.*[29] and Tuttle and Adams[31] do allow bulk diffusion of H by first creating a liquid sample of the material and then quenching it, a procedure that has known shortcomings, such as overcoordination, no definite gap, etc.

Specifically, the plane wave MD Car-Parrinello method was applied to amorphous hydrogenated silicon by Buda *et al.*[29] using a cubic cell of 64 silicons and 8 hydrogens (11% concentration). They start out with a liquid material containing both silicon and hydrogen atoms that is rapidly quenched, maintaining a density equal to the value of the crystalline material. They report only partial distribution functions and, as is usually the case, the H-H RDF is poorly reproduced and is not compared to the existing experimental neutron diffraction data. The DFT-LDA approach of Sankey and coworkers was applied to this material by Fedders and Drabold[30] using several cells based on a two-defect 63 silicon atom supercell that was constructed in previous work.[24,26] The hydrogen was introduced into the amorphous silicon sample by hand so that the H-atoms are located near (1.5 Å) the corresponding dangling bond. To eliminate the strained bond defects they removed the silicon considered to be the center of the strain defect and put H atoms

near the 4 dangling bonds. Posterior relaxation allowed the hydrogens to be trapped by the dangling bonds. Fedders and Drabold[30] do not report any RDF, total or partial. Tuttle and Adams[31] also use the Harris functional in the DFT-LDA code developed by Sankey *et al.* and apply it to a cell of 242 atoms with 11% hydrogen. They generate the structure from a liquid at $\approx$ 1800 K and quench it to produce an amorphous structure at 300 K. Since they were not concerned with real time dynamics, they set the mass of hydrogen equal to the mass of Si, thereby allowing the use of a large time step in the annealing process (4 fs). However, this means that the RDFs could not reflect real diffusion processes of the hydrogens in the cell, and correspondingly only the Si-Si and the Si-H RDFs are reported. A significant percentage of defects with only 90% of the silicon being fourfold coordinated is found.

Even though tight binding calculations have been labeled as "highly arbitrary and inadequate",[26] some of them deserve special mention. Biswas *et al.*[34] using this approach studied the electronic structure of dangling and floating bonds in amorphous silicon. Fedders[35] looked into the energetics of defects and found that tight binding gives surprisingly good results for the energy eigenvalues and the degree of localization of the defect states if some radial dependence is included in the hopping matrix elements. Colombo and Maric[36] reported the first tight-binding molecular-dynamics simulation of the defect-induced crystal-to-amorphous transition in crystalline silicon. In particular, two recent ones are specially relevant for the present work: Yang and Singh[37] find that the total average energy per silicon atom is a minimum when the hydrogen concentration is in the range 8-14%, the optimum experimental range found; Klein *et al.*[38] report a H-H RDF closer to experimental results than previous work. Both studies start out from liquid samples that are fast quenched to generate the hydrogenated amorphous silicon and therefore, as in all other cases, a large percentage of defects, floating or dangling bonds, are naturally created. For a recent account of the state of the art of tight binding methods see Ref. 39 where both parameterized and *ab initio* approaches are considered.

III. METHOD

In this work we report the generation of samples of both *a*-Si and *a*-Si:H using a new approach (with four different time steps) that leads to structures with a minimum of coordination defects. We use *FastStructure*,[40] a DFT code based on the Harris functional, and optimization techniques based on a fast force generator to allow simulated annealing/molecular dynamics studies with quantum force calculations.[41] We use the LDA parameterization due to Vosko, Wilk and Nusair (VWN)[42] in the simulations. The core is taken as full which means that an all electron calculation is carried out, and for our simulations a minimal basis set of atomic orbitals was chosen with a cutoff

radius of 5 Å, (compare to values of ≈ 2.6 Å used by Sankey *et al.*), a compromise between cost and accuracy. The physical masses of hydrogen and silicon are used throughout and this allows us to see realistic diffusive processes of the hydrogen atoms in the supercell. The default time step is given by $\sqrt{m_{min}/5}$, where m_{min} is the value of the smallest mass in the system; however, in order to better simulate the dynamical processes that occur in the amorphisation a time step of 10 fs (compare to 2.44 fs, the default value) was also used for the pure silicon and 2 fs was used when hydrogen was introduced, in addition to 0.46 fs, the default time step. The forces are calculated using rigorous formal derivatives of the expression for the energy in the Harris functional, as discussed by Lin and Harris.[43] The evaluation of the 3-center integrals that contribute to the matrix elements in the one-particle Schrodinger equation is the time-limiting feature of *FastStructure* and each is performed using the weight-function method of Delley.[44]

Since it is clear that quenching from a melt or from partially melted samples generates undesirable structures, we took a different path. Our process, like the ones mentioned above, is not designed to reproduce the way an amorphous material is grown, but has the objective of generating an amorphous sample that would represent adequately the ones obtained experimentally. We amorphisized the crystalline diamond structure with 64 silicon atoms in the cell (a crystalline density of 2.33 g/cm^3) by slowly heating it from room temperature to well above the glass transition temperature and just below the melting point, and then slowly cooling it to 0 K. This then was followed by cycles of annealing and quenching at temperatures suggested by experiment, to let the structure obtained adjust to the local energy minimum. Heating, cooling, annealing and quenching cycles were carried out using either the 2.44 fs or the 10 fs time step throughout.

To treat *a*-Si:H we first constructed two amorphous silicon structures as follows: One was created as described above, with a time step of 2.44 fs, maintaining the crystalline density, and then expanded to reproduce the experimental density, 2.2 g/cm^3 of the hydrogenated structure, once hydrogens are incorporated. The other was created using a time step of 10 fs from an expanded crystalline cell so that the density of the hydrogenated cell (2.2 g/cm^3) corresponds to the reported experimental values. Once these expanded pure amorphous silicon cells were constructed, we introduced 12 hydrogen atoms at the following relative cell positions: (1/4, 1/4, 1/4), (3/4, 1/4, 1/4), (3/4, 3/4, 1/4), (1/4, 3/4, 1/4), (1/2, 1/4, 1/2), (3/4, 1/2, 1/2), (1/2, 3/4, 1/2), (1/4, 1/2, 1/2), (1/4, 1/4, 3/4), (3/4, 1/4, 3/4), (3/4, 3/4, 3/4), (1/4, 3/4, 3/4), and annealed them at temperatures suggested by experiment.

Specifically, for *a*-Si the cell was heated from 300 K to 1,680 K, just below the melting temperature of crystalline silicon, in 100 steps of 10 fs, and immediately cooled down to 0 K in 122 steps of 10 fs; this was done also for a time step of 2.44 fs. The heating/cooling rate was 5.66×10^{15}K/s for 2.4 and 1.38×10^{15}K/s for 10 fs, approximately. The

atoms were allowed to move freely within each cell of volume (10.8614 Å)^3 with periodic boundary conditions. Once this first stage was complete, we subjected each cell to annealing cycles at 300 K (below microcrystallization[8]) with intermediate quenching processes.

For *a*-Si:H we implemented two different procedures. First, we used the amorphous pure silicon cell generated above with a time step of 2.44 fs and then expanded it to a volume of (11.0620 Å)^3. Second, we amorphisized a previously expanded crystalline cell of 64 silicon atoms with the same volume of (11.0620 Å)^3 using a 10 fs time step and repeating the cycles described above. We then placed the 12 hydrogens distributed throughout the amorphous cells and subjected the system to annealing cycles using a time step of 0.46 fs for the first cell (the 2.44/0.46 cell), and 2 fs for the second one (the 10/2 cell). The annealing cycles consist of two cycles of 50 steps at 300 K for the large time step sample and one cycle of 200 steps for the small time step sample, with in between quenches down to 0 K, to allow the hydrogens to diffuse and move in the cells. This gives a concentration of hydrogen of practically 16%, adequate to compare with existing experimental results.

Once the atomic structures were constructed and their respective RDFs obtained, we analysed their electronic density of states at the Γ point of the Brillouin Zone using both *FastStructure* and the DFT approach of Hohenberg and Kohn[45] and Kohn and Sham[46] implemented in the *ab initio DMol3* comercial code;[47] both codes were used to calculate the energy levels and DOS curves of the amorphous atomic structures generated. *DMol3* treats the electronic structure of periodic solids by solving the Kohn-Sham self-consistency equations within local or nonlocal density approximations; in our work we carried out just energy calculations of the structures found with *FastStructure* and used the LDA approximation. We also used a double numerical basis set that includes *d*-polarization of the atoms (DNP) and the frozen inner core orbitals approximation; a medium grid was used for the numerical calculations. The SCF density parameter that specifies the degree of convergence for the LDA density was set at 10^{-6}. The HOMOs, LUMOs and DOS curves were calculated since they are necessary to study the behaviour of the forbidden energy gaps, the position of the Fermi levels, and the gap levels introduced by either dangling bonds, floating bonds or hydrogen states.

IV. RESULTS AND DISCUSSION

Defining a dangling or a floating bond is to some extent arbitrary since one has to choose some interatomic distance; Drabold *et al.*[24] chose an interatomic distance of 2.7 Å, although no clear justification for this choice is given. Lee and Chang[28] use the distance at which the minimum of the RDF occurs, 2.73 Å, which leads to an average number

of nearest neighbors in the amorphous cell of 3.9. Were we to use the minimum value of the RDF of Fedders *et al.*,[26] $\approx 1.2 \times 2.35 = 2.82$ Å, it is certain that the number of defects reported by Drabold and coworkers would have changed significantly. An analysis of structural defects *versus* spectral defects was performed by these authors and it was concluded that dangling bonds give rise to defects within the gap, that some strained tetrahedral structures may also generate gap states, but that it seems floating bonds do not create gap states. Recent work, however, indicates that floating bonds may generate gap states,[48] and this conclusion is also borne out in the results reported here.

Generating a clean gap in such small cells is a difficult task since defects always appear in the simulations; so it seems that the most one can hope for is to minimize the number of defects and so obtain a reasonably clean electronic gap. On the other hand, generating RDFs, total and partial, that compare favorably with experiment is very important as is reproducing the hydrogen dynamics and its experimental behaviour of passivating the dangling bonds in amorphous silicon. This 'cleans' the gap, in spite of the limited size of the cells. Herein we address these issues and report total RDFs for pure and hydrogenated amorphous silicon, and partial RDFs for silicon-silicon, silicon-hydrogen and hydrogen-hydrogen in the hydrogenated samples and also report HOMOs, LUMOs and their DOS curves.

A. The atomic structure

For *a*-Si the RDF obtained from our simulation with 10 fs agrees very well with experiment from 0 to 10 Å, Fig. 1. In this work we fourier-smoothed all the RDF results to have adequate curves to allow comparison with experiment, since the small number of atoms in the cell leads to statistical fluctuations that are not representative of the bulk. In Fig. 1 we do a direct comparison of our results and the upper and lower experimental bounds from Refs. 10 to 16 and, considering that not all experimental results cover the range 0 to 10 Å, the agreement is excellent, including the existence and position of the third and the fourth amorphous peaks. The evolution of the crystalline peaks can be clearly observed in our simulations, Fig. 2, and we can say that the first crystalline peak remains as the most prominent feature in the amorphous material. The second crystalline peak also remains but is widened and highly diminished since it contributes to filling in the first and second crystalline valleys. The third crystalline peak disappears to contribute to the valleys between the second and third and the third and fourth crystalline peaks, and the fourth crystalline peak disappears to contribute to the filling in the valleys between the third and fifth crystalline peaks. The fifth crystalline peak generates a third amorphous peak slightly displaced to smaller distances. This figure presents a comparison of the position of the crystalline peaks and the amorphous structure where all this can be

better appreciated.

The total and partial RDF simulations for *a*-Si:H also compare very favorably with the experimental results given in Ref. 18, where a more complete and more recent study is reported. In Figs. 3 and 4 we show the comparison of the total RDFs and the partial H-H RDFs with experiment for the two cells, 2.44/0.46 (Fig. 3) and 10/2 (Fig. 4), where the peak due to the presence of molecular hydrogen that appears in the simulation of the 10/2 cell has been removed in order to better illustrate the agreement of our results with experiment. In particular, the H-H correlation function that we obtained for the 2.44/0.46 fs cell is close to the experimental results of Bellissent *et al.*[17] unlike previous *ab initio* simulations. As we shall see later, it turns out that this sample contains more dangling and floating bonds than the 10/2 fs cell. Since the number of hydrogen atoms in the cells is smaller than the number of silicon atoms, a larger fourier smoothing for the H-H partial was used in order to compare our results with experiment. In Fig. 5 we are able to see the dynamics of the originally evenly distributed hydrogen (see Fig. 6 for the distribution of hydrogens) since for the 10/2 fs cell a peak appears in the total and H-H RDFs due to the formation of molecular hydrogen at an interatomic distance of 0.875 Å, (see Ref. 49 where a molecular radius of 0.86 Å for hydrogen in a crystalline silicon cluster is reported). No formation of molecular hydrogen shows up in the 2.44/0.46 fs cell since the large number of dangling bonds inhibits it. Figs. 7 to 10 depict four structures that clearly indicate the passivation process of the existing dangling bonds in the pure amorphous silicon samples due to hydrogenation: Fig. 7(9) shows 5(2) dangling bonds that existed in the pure amorphous sample for the 2.44(10) fs cell, for a cutoff radius of 2.815(2.743) Å below which the number of neighbors is 4(4); Fig. 8(10) shows the 2.44/0.46(10/2) fs cells indicating that 3(1) bonds were passivated by hydrogens, 2(1) by silicons, and 3(2) new ones appeared; here the same cutoff radius mentioned above for Si-Si was used, whereas the cutoff radius for Si-H was 1.9(1.9) Å which is the position of the valley minimum between the first and second peaks in the Si-H partial RDF (See Figs. 11 and 12). The Si-Si and Si-H partial RDF also agree well with experiment, as indicted in Figs. 11 and 12 where a direct comparison is shown.

The 2.44/0.46 cell shows a large number of floating bonds, 11, after the hydrogen diffusion process, as opposed to 3 floating bonds (fb) for the 10/2 fs cell. Of the 11 fb, 6 are due to hydrogen atoms that bond to silicons in addition to the existing tetrahedral coordination and it is for this cell that the addition of H decreases the size of the electronic gap, as will be shown next, indicating the important role of this type of bonds in reducing the gap.

B. The electronic density of states

Using *ab initio* methods in order to study electronic characteristics of amorphous materials invariably forces one to consider cells of some hundred atoms at most, due to the limitations in computing power of present day resources. Therefore it is desirable to have practically no defects in these cells since then they would better represent what occurs in the best extended samples. However, as stated before, simulations in cells of 64 to 216 atoms usually have a large concentration of dangling and floating bonds. That is why we have developed a different approach to generate amorphous cells that seem to give a smaller concentration of these defects and that are therefore more in agreement with good bulk samples.

As mentioned above for *a*-Si our two amorphous cells 2.44/10 have 5 and 3 dangling bonds and 5 and 1 floating bonds for a cutoff radius of 2.763/2.772 Å. At these distances the number of nearest neighbors (area under the first amorphous peak) is equal to 4. Calculations of the DOS curves, and HOMOs and LUMOs with both *FastStructure* and *DMol3* give clean gaps of 0.414 eV and 0.173 eV respectively for the 2.44 fs cell and 0.744 eV and 0.385 eV respectively for the 10 fs cell . The gaps were obtained just by looking at the HOMO and LUMO values; no attempt was made at sorting out the states near the gap due to dangling and/or floating bonds. Figs. 13 and 14 show the DOS curves where the gaps are clearly indicated. It should be kept in mind that density functional calculations using the local density approximation tend to underestimate band gaps.

Two procedures were carried out in order to generate the amorphous cells of hydrogenated silicon of the correct density; both imply an expansion of the cell either before the amorphisation or after, as described above. When the cell is expanded after the amorphisation a larger number of defects is created, 6 dangling bonds and 2 floating bonds, for the cutoff radius of 2.763 Å. Then 12 hydrogens were placed as described above and indicated in Fig. 6 and the cell was annealed as described above. It should be emphasized that in this method the hydrogen atoms were left free to diffuse, unlike other results reported in the literature where the hydrogens are placed in *ad hoc* positions to saturate the dangling bonds. Figs. 15 and 16 show the DOS curves obtained with *FastStructure* and *DMol3* for hydrogenated amorphous silicon, the gap values are 0.324 eV and 0.142 eV for the 2.44/0.46 fs cell and 0.787 eV and 0.483 eV for the 10/2 fs cell, respectively. The result obtained with the 10/2 fs cell follows the trend found in experiments that the addition of hydrogen increases the gap value with respect to pure silicon. The result for the 2.44/0.46 fs cell indicate that the size of the gap can be diminished by the presence of the 6 hydrogen-related and 5 silicon-related floating bonds; this supports the idea expressed recently by Fornary and coworkers.[48]

V. CONCLUSIONS

Dealing theoretically with a covalent amorphous material in bulk is difficult because there are many possible structures for a given RDF. Continuous random-network models have achieved considerable success in generating a-Si structures but these models are not easily generalizable to other glassy materials or systems with different species of atoms. That is why the simulation of covalent amorphous semiconductors in the bulk, both pure and alloyed, has encountered serious obstacles. In the present work, we have been able to perform *ab initio* simulations of the atomic structure and electronic features of amorphous pure and hydrogenated silicon and simulation of their total and partial atomic RDFs that reproduce many features shown by the experimental data. In particular, our RDFs agree very well with the corresponding experimental distributions up to the third and fourth peaks, as can be seen in the direct comparisons made in the figures. In addition, the dynamics of atomic hydrogen, including the formation of molecular hydrogen under certain conditions, and the passivation of dangling bonds was observed. The electronic density of states of the atomic distributions generated indicate the presence of a gap for the pure amorphous silicon samples that widens when the sample is annealed after hydrogen is distributed within the cell and the number of defects (dangling and floating bonds) is kept low.

The procedure that we used to generate these structures is different from the ones found in the literature and leads to amorphous samples with fewer dangling bonds and fewer overcoordinated defects. It consists of heating a crystalline sample of 64 atoms of silicon just below its melting temperature and then cooling it down to 0 K with subsequent annealing and quenching cycles at temperatures dictated by experiment.

We believe that our procedure can be generalized to other monatomic or diatomic amorphous semiconducting materials and therefore allows *ab initio* techniques to be used in other areas to provide more representative structures and a more complete description of their atomic and electronic characteristics than is possible with parameterized methods. Furthermore, *ab initio* simulations can be used to provide the parameters needed in non *ab initio* techniques to be able to handle larger amorphous cells.

ACKNOWLEDGMENT

AAV thanks DGAPA-UNAM for financial support to spend a sabbatical year at *Molecular Simulations, Inc.* where this work was begun and for financial support to carry out this research through project IN101798 (*Estructura Electrónica y Topología Atómica de Silicio Amorfo Puro y Contaminado*). FA thanks CONACyT for supporting his PhD studies. This work was done on an Origin 2000 computer provided by DGSCA, UNAM.

* Corresponding author; e-mail: valladar@servidor.unam.mx

[1] G. Szekely, J. Electrochem. Soc. **98**, 318 (1951).

[2] H. Richter and G. Breitling, Z. Naturf.**13**a, 988 (1958), and work cited therein.

[3] R. Grigorovici and R. Manaila, Thin Solid Films **1**, 343 (1968).

[4] M.V. Coleman and D.J.D. Thomas, Phys. Stat. Solidi **25**, 241 (1968).

[5] A.A. Valladares, A. Valladares, R.M. Valladares and M.A. Mc Nelis, J. Non-Cryst. Solids, **231**, 209 (1998). R.M. Valladares, C.C. Díaz, M. Arroyo, M.A. Mc Nelis and Ariel A. Valladares, Phys. Rev. B **62**, 2 220 (2000).

[6] N.F. Mott and E.A. Davis, *Electronic Processes in Non-crystalline Materials*, Oxford University Press, 1971; p. 272.

[7] W.E. Spear and P.G. Le Comber, Solid State Commun. **17**, 9 (1975).

[8] R. A. Street, *Hydrogenated Amorphous Silicon*, Cambridge University Press, 1991.

[9] T.A. Postol, C.M. Falco, R.T. Kampwirth, I.K. Schuller and W.B. Yelon, Phys. Rev. Lett. **45**, 648 (1980).

[10] S.C. Moss and J.F. Graczyk, Phys. Rev. Lett. **23**, 1 167 (1969), and *Proceedings of the 10th International Conference on the Physics of Semiconductors*, Cambridge, MA, (ed. S.P. Keller, J.C. Hensel and F. Stern), 1970, p. 658. United States Atomic Energy Comission.

[11] A. Barna, P.B. Barna, G. Radnóczi, L. Tóth and P. Thomas, Phys Stat. Sol. **A41**, 81 (1977).

[12] R. Mosseri, C. Sella and J. Dixmier, Phys Stat. Sol. **A52**, 475 (1979).

[13] J. Fortner and J.S. Lannin, Phys. Rev. B**39**, 5 527 (1989).

[14] S. Kugler, G. Molnár and A. Menelle, Phys. Rev. B**40**, 8 030 (1989).

[15] S. Kugler, L. Pustai and L. Rosta, Phys. Rev. B**48**, 7 685 (1993).

[16] K. Laaziri, S. Kycia, S. Roorola, M. Chicoine, J.L. Robertson, J. Wang and S.C. Moss, Phys. Rev. Lett. **82**, 3460 (1999).

[17] R. Bellissent, A. Chenevas-Paule, P. Chieux and A. Menelle, J. Non-Cryst. Solids **77-78**, 213 (1985).

[18] R. Bellissent, A. Menelle, W.S. Howells, A.C. Wright, T.M. Brunier, R.N. Sinclair and F. Jansen, Physica B**156-157**, 217 (1989).

[19] J.L. Feldman, S.R. Bickham, G.E. Engel and B.N. Davidson, Phil. Mag. B, **77**, 507 (1998).

[20] E. Roger Cowley, Phys. Rev. Lett. **60**, 2 379 (1988). See also D.A. Drabold, P.A. Fedders, A.E. Carlsson O.F. Sankey and J.D. Dow, Phys. Rev. B**42**, 5 345 (1990).

[21] I. Kwon, R. Biswas, C.Z. Wang, K.M. Ho and C.M. Soukoulis, Phys. Rev. B**49**, 7 242 (1994).

[22] Q. Li and R. Biswas, Phys. Rev. B**50**, 18 090 (1994).

[23] R. Car and M. Parrinello, Phys. Rev. Lett. **60**, 204 (1988).

[24] D.A. Drabold, P.A. Fedders, O.F. Sankey and J.D. Dow, Phys. Rev. B**42**, 5 135 (1990).

[25] I. Stich, R. Car and M. Parrinello, Phys. Rev. B**44**, 11 092 (1991).

[26] P.A. Fedders, D.A. Drabold and S. Klemm, Phys. Rev. B**45**, 4 048 (1992).

[27] F. Wooten, K. Winer and D. Weaire, Phys. Rev. Lett. **54**, 1 392 (1985).

[28] I. Lee and K.J. Chang, Phys. Rev. B, **50**, 18 083 (1994).

[29] F. Buda, G.L. Chiarotti, R. Car and M. Parrinello, Phys. Rev. B**44**, 5 908 (1991).

[30] P.A. Fedders and D.A. Drabold, Phys. Rev. B**47**, 13 277 (1993).

[31] B. Tuttle and J.B. Adams, Phys. Rev. B**53**, 16 265 (1996).

[32] O.F. Sankey and D.J. Niklewsky, Phys. Rev. B**40**, 3979 (1989), O.F. Sankey and D.A. Drabold, Bull. Am. Phys. Soc. **36**, 924 (1991).

[33] J. Harris, Phys. Rev. B**31**, 1770 (1985).

[34] R. Biswas, C.Z. Wang, C.T. Chan, K.M. Ho and C.M. Soukoulis, Phys. Rev. Lett. **63**, 1 491 (1989).

[35] P.A. Fedders, J. Non-Cryst. Solids **137&138**, 141 (1991).

[36] L. Colombo and D. Maric, Europhys. Lett. **29**, 623 (1995).

[37] R. Yang and J. Singh, J. Non-Cryst. Solids **240**, 29 (1998).

[38] P. Klein, H.M. Urbassek and T. Frauenheim, Phys. Rev. B**60**, 5 478 (1999).

[39] *Tight-Binding Approach to Computational Materials Science*, MRS Symposium Proceedings Volume 491, ed. P.E.A. Turchi, A. Gonis and L. Colombo, 1998. Materials Research Society, Warrendale PA., USA.

[40] *FastStructure_SimAnn, User Guide*, Release 4.0.0 (San Diego, Molecular Simulations, Inc., September 1996).

[41] Xiao-Ping Li, J. Andzelm, J. Harris and A.M. Chaka, American Chemical Society, Anaheim Symposium [Ed. Ziegler], Chapter 26, (1996).

[42] S.H. Vosko, L. Wilk and M. Nusair, Can. J. Phys. **58**, 1200 (1980).

[43] Z. Lin and J. Harris, J. Phys. Condens. Matter, **5** 1055 (1992).

[44] B. Delley, J. Chem. Phys., **92**, 508 (1990).

[45] P. Hohenberg and W. Kohn, Phys. Rev. B **136**, 864 (1964).

[46] W. Kohn and L.J. Sham, Phys. Rev. A **140**, 1133 (1965).

[47] *Quantum Chemistry, DMol3 User Guide*, Cerius2-3.5, Molecular Simulations, Inc., San Diego, 1996. See also B. Delley, J. Chem. Phys. **92**, 508 (1990); **94**, 7245 (1991).

[48] M. Fornari, M. Peressi, S. de Gironcoli and A. Baldereschi, Europhys. Lett., **47**, 481 (1999).

[49] K.G. Nakamura, K. Ishioka, M. Kitajima and K. Murakami, Solid State Comm., **101**, 735 (1997).

FIGURE LIST

FIG. 1. RDFs for *a*-Si. The lighter lines are the experimental upper and lower bounds (see text). The dark line is our simulation where the third and fourth peaks are well reproduced.

FIG. 2. Evolution of the crystalline peaks during amorphisation. The RDF for *a*-Si (dark line) has four well defined peaks that are generated by several crystalline peaks (lighter vertical lines).

FIG. 3. Direct comparison of the simulated (dark lines) total RDF for *a*-Si:H and partial RDF for H-H (Inset) (with 15.79% hydrogen concentration) to the experimental (light lines) results for the short time steps cell (2.44/0.46 fs).

FIG. 4. Direct comparison of the simulated (dark lines) total RDF for *a*-Si:H and partial RDF for H-H (Inset) (with 15.79% hydrogen concentration) to the experimental (light lines) results for the long time steps cell (10/2 fs). The peak due to molecular hydrogen has been removed for clarity.

FIG. 5. Total RDF for the 10/2 fs cell of hydrogenated amorphous silicon (dark line) that shows the presence of molecular hydrogen, compared to the experimental results (light line).

FIG. 6. Starting positions of the 12 hydrogens placed within the amorphous cells of pure silicon. The relative coordinates are given in the text.

FIG. 7. Short time step cell of pure amorphous silicon (2.44 fs) that shows the existence of 5 dangling bonds. A cutoff radius of 2.815 Å was used, below which the total number of nearest neighbors is 4.

FIG. 8. When hydrogen is added to the short time steps cell, and the sample annealed, 3 dangling bonds are passivated by hydrogens and 2 by silicons but 3 new ones appear; however, 11 new floating bonds are formed (not shown).

FIG. 9. Long time step cell of pure amorphous silicon (10 fs) that shows the existence of 2 dangling bonds. A cutoff radius of 2.743 Å was used, below which the total number of nearest neighbors is 4.

FIG. 10. When hydrogen is added to the long time steps cell, and the sample annealed, all dangling bonds (2) are passivated, one by hydrogen and one by silicon, and 2 new ones appear. The number of floating bonds now is only 3 (not shown). The appearance of molecular and atomic hydrogen is indicated.

FIG. 11. Partial Si-Si and Si-H RDFs for the hydrogenated short time steps cell. The simulated results are represented by dark lines whereas the experimental ones are represented with lighter lines.

FIG. 12. Partial Si-Si and Si-H RDFs for the hydrogenated long time steps cell. The simulated results are represented by dark lines whereas the experimental ones are represented with lighter lines.

FIG. 13. DOS curves for the 2.44 fs cell of *a*-Si calculated using *FastStructure*, curve (a), and *DMol3*, curve (b). HOMOs and LUMOs are shown that lead to a gap of 0.414 eV for (a) and 0.173 eV for (b).

FIG. 14. DOS curves for the 10 fs cell of *a*-Si calculated using *FastStructure*, curve (a), and *DMol3*, curve (b). HOMOs and LUMOs are shown that lead to a gap of 0.744 eV for (a) and 0.385 eV for (b).

FIG. 15. DOS curves for the 2.44/0.46 fs cell of *a*-Si:H calculated using *FastStructure*, curve (a), and *DMol3*, curve (b). HOMOs and LUMOs are indicated and the gap values are 0.324 eV and 0.142 eV, respectively.

FIG. 16. DOS curves for the 10/2 fs cell of *a*-Si:H calculated using *FastStructure*, curve (a), and *DMol3*, curve (b). HOMOs and LUMOs are indicated and the gap values are 0.787 eV and 0.483 eV, respectively.

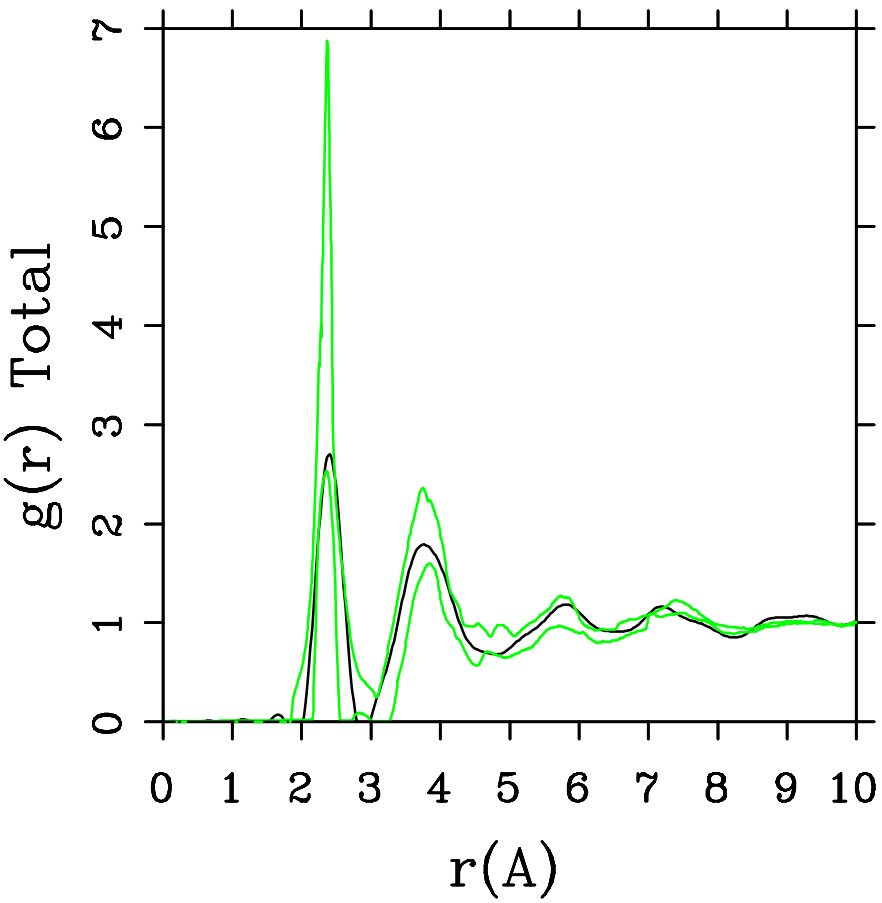
g(r) Total
0
1
2
3
4
5
6
7
0
1
2
3
4
5
6
7
8
9
10
r(A)

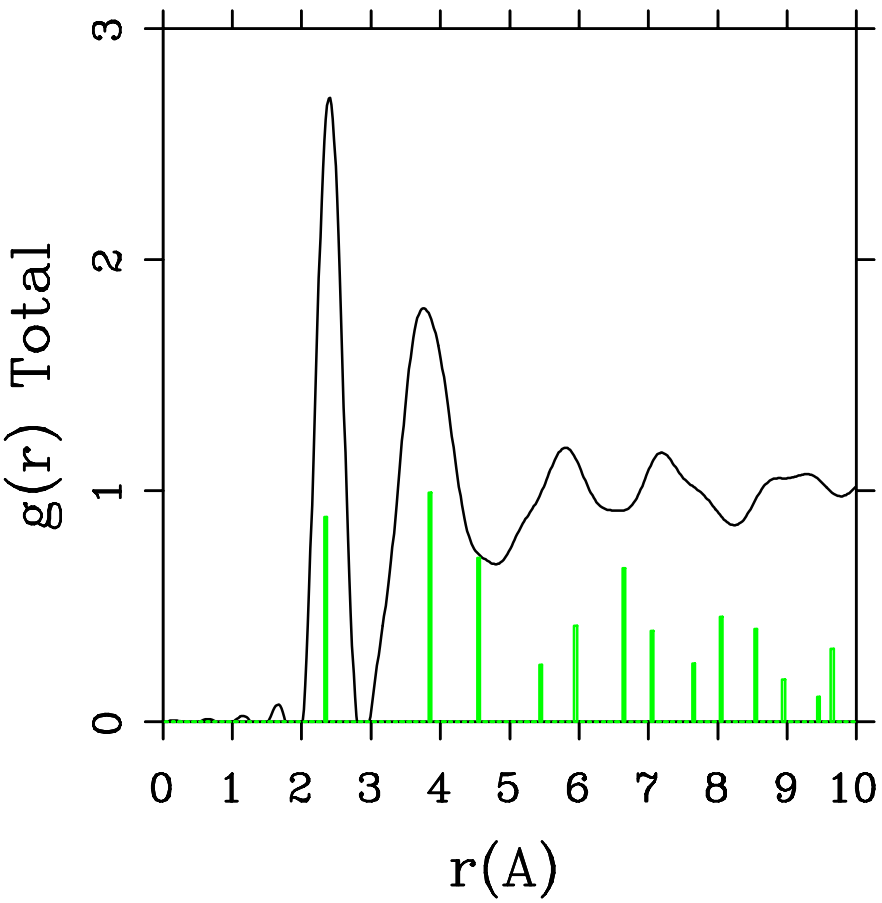
g(r) Total
0
1
2
3
0
1
2
3
4
5
6
7
8
9
10
r(A)

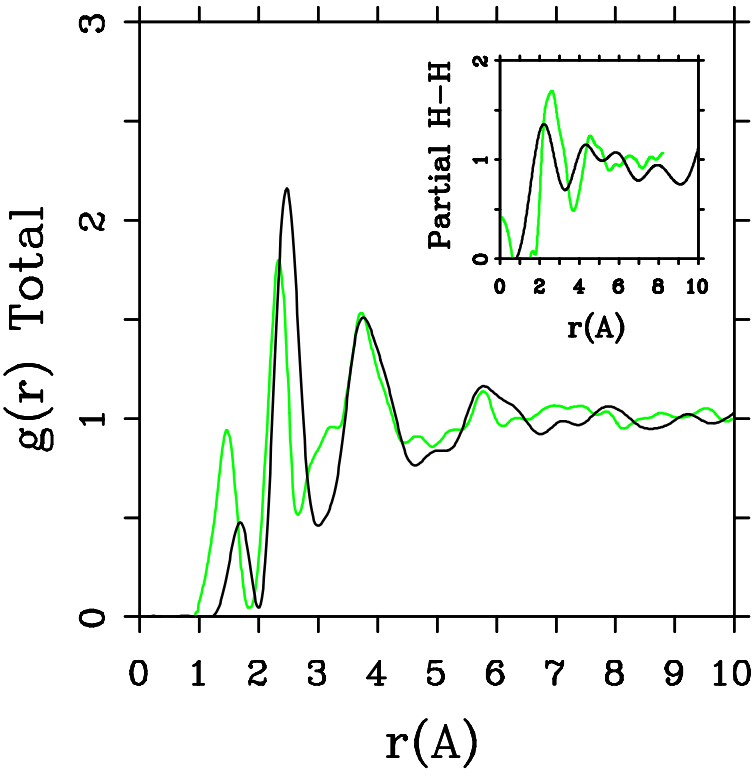
g(r) Total
r(A)
Partial H-H
r(A)

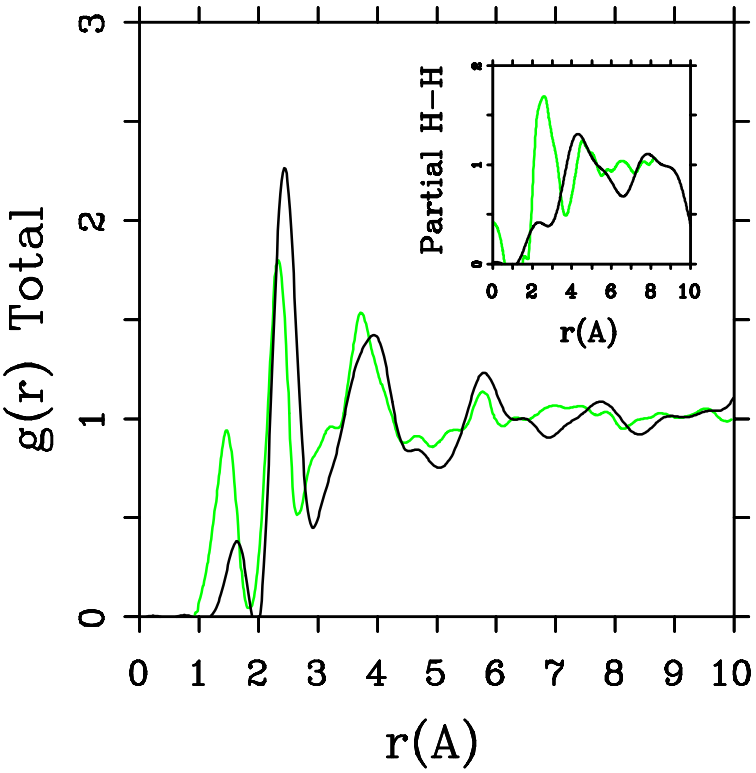
g(r) Total
r(A)
Partial H-H
r(A)

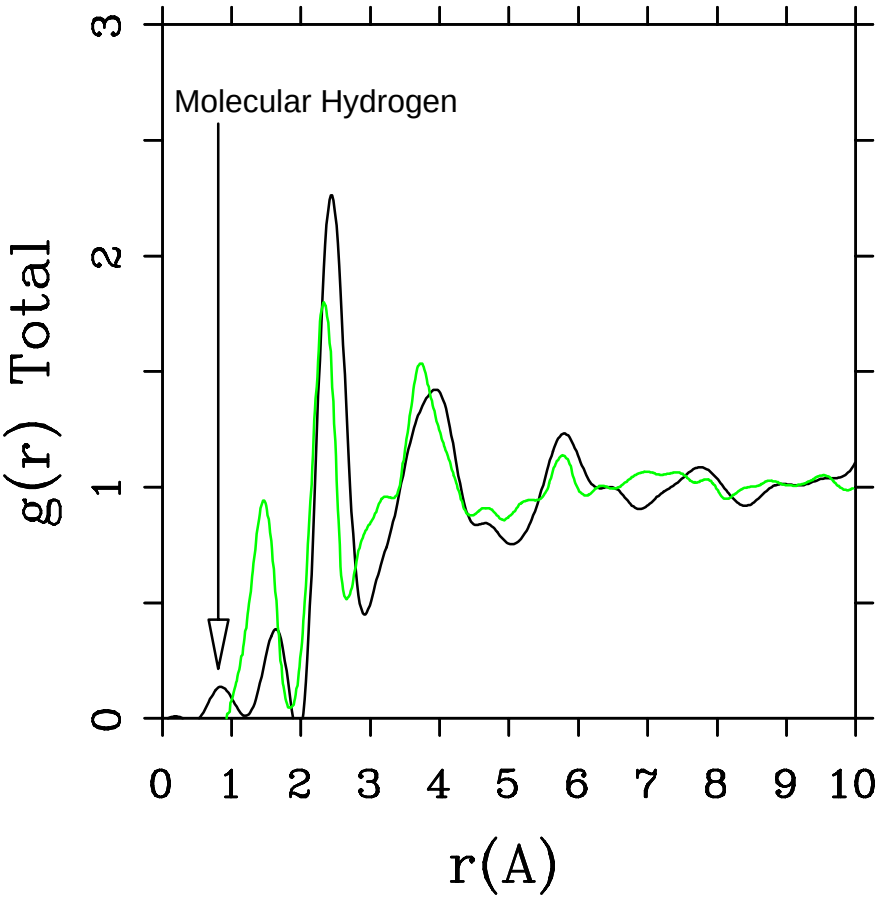
Molecular Hydrogen
g(r) Total
r(A)
0
1
2
3
0
1
2
3
4
5
6
7
8
9
10

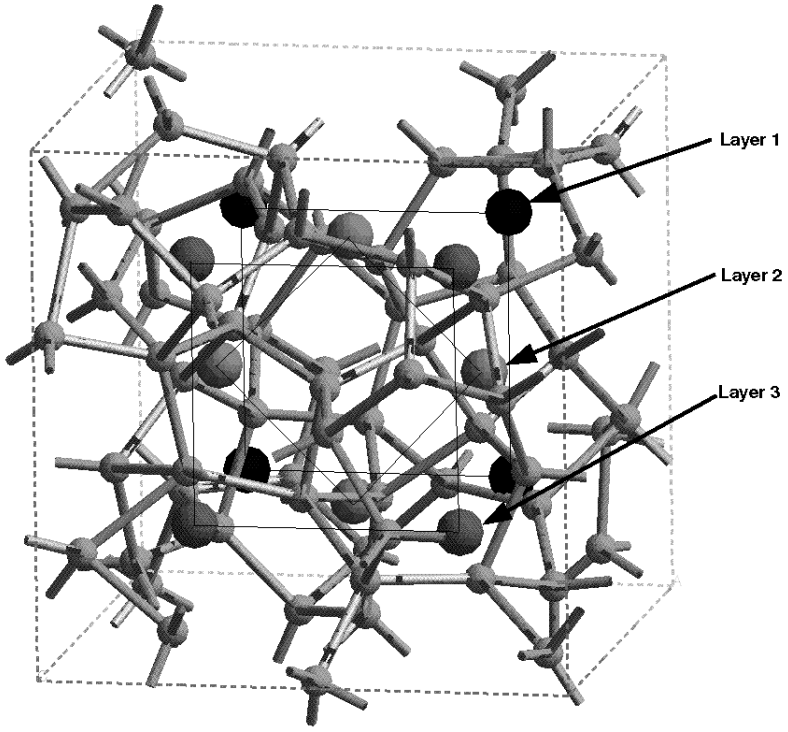
Layer 1
Layer 2
Layer 3

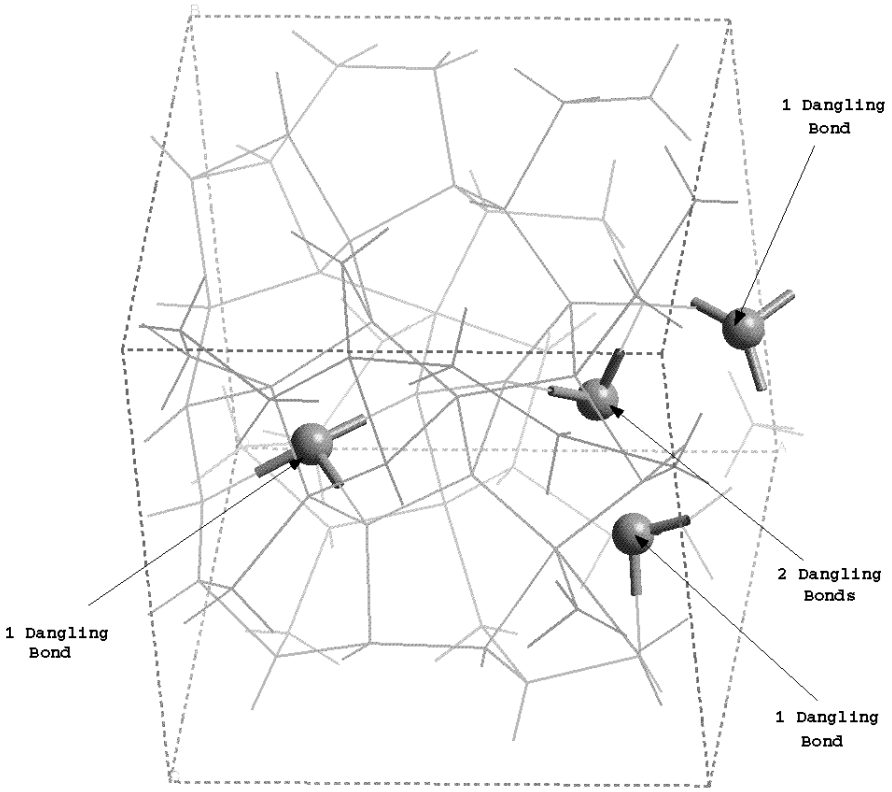
1 Dangling
Bond
2 Dangling
Bonds
1 Dangling
Bond
1 Dangling
Bond

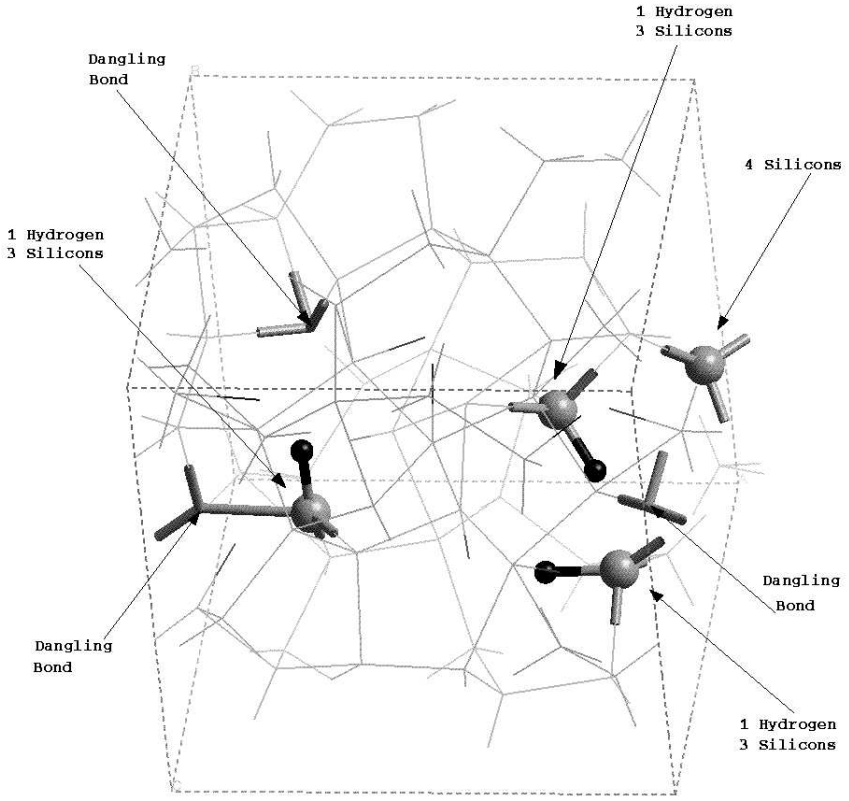
1 Hydrogen
3 Silicons
Dangling
Bond
4 Silicons
1 Hydrogen
3 Silicons
Dangling
Bond
Dangling
Bond
1 Hydrogen
3 Silicons

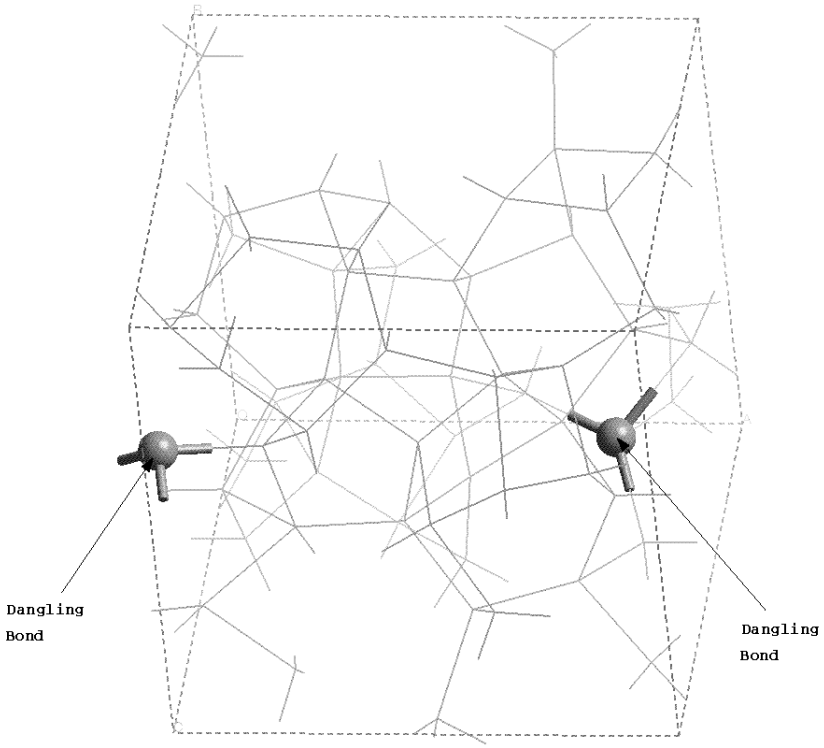
Dangling
Bond
Dangling
Bond

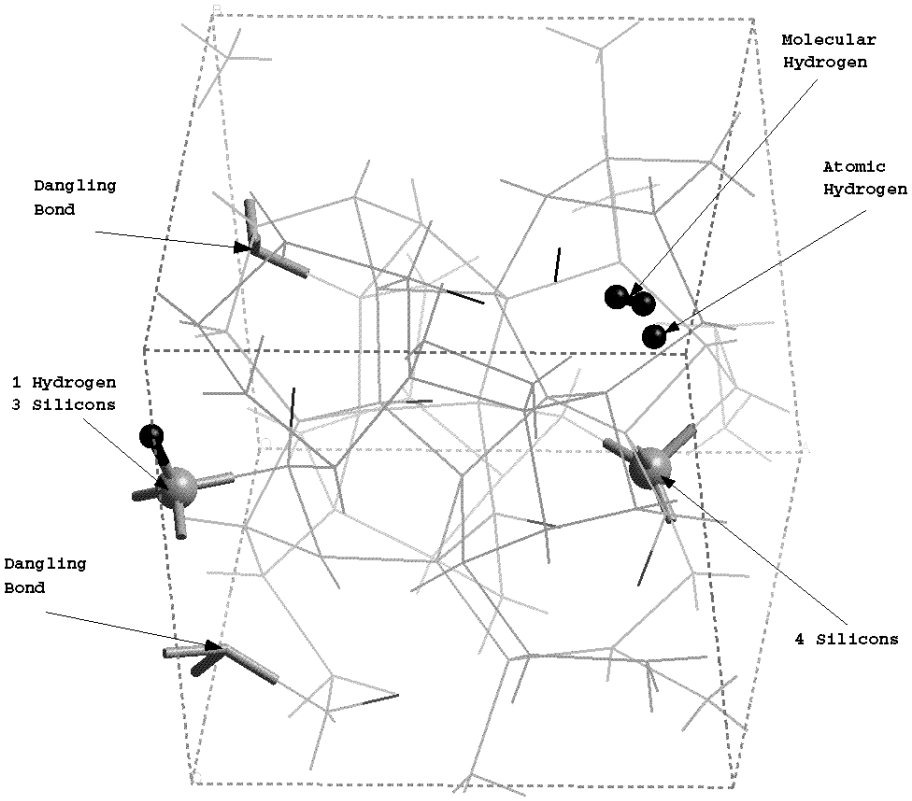
Molecular
Hydrogen
Atomic
Hydrogen
Dangling
Bond
1 Hydrogen
3 Silicons
Dangling
Bond
4 Silicons

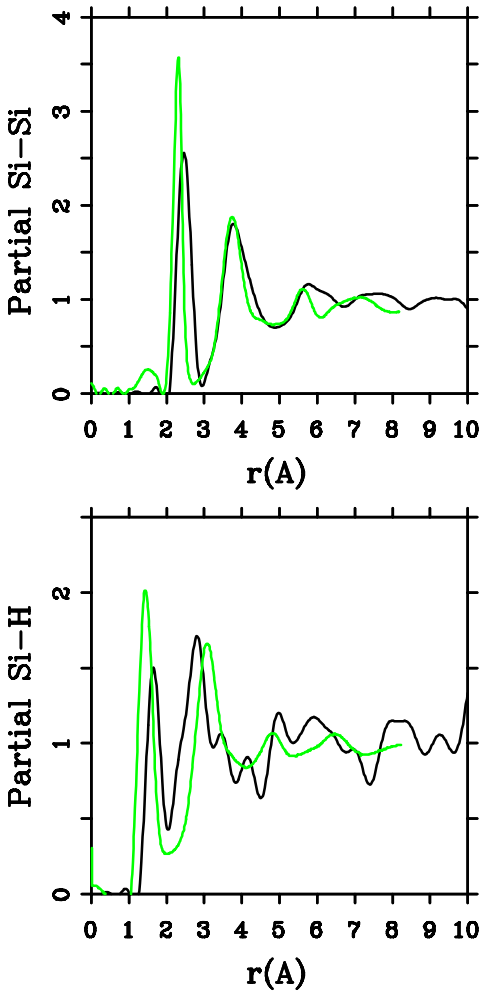
Partial Si-Si
0
1
2
3
4
0 1 2 3 4 5 6 7 8 9 10
r(A)
Partial Si-H
0
1
2
0 1 2 3 4 5 6 7 8 9 10
r(A)

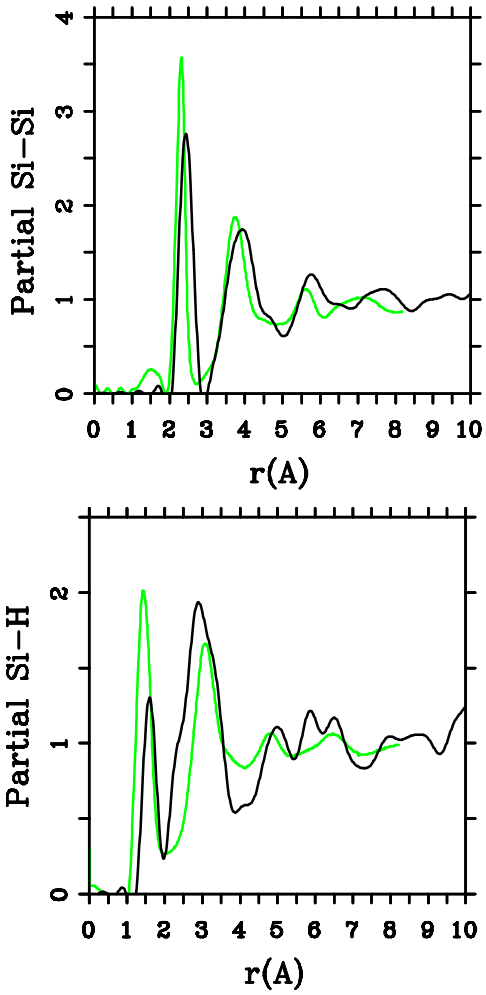
Partial Si-Si
0
1
2
3
4
0 1 2 3 4 5 6 7 8 9 10
r(A)
Partial Si-H
0
1
2
0 1 2 3 4 5 6 7 8 9 10
r(A)

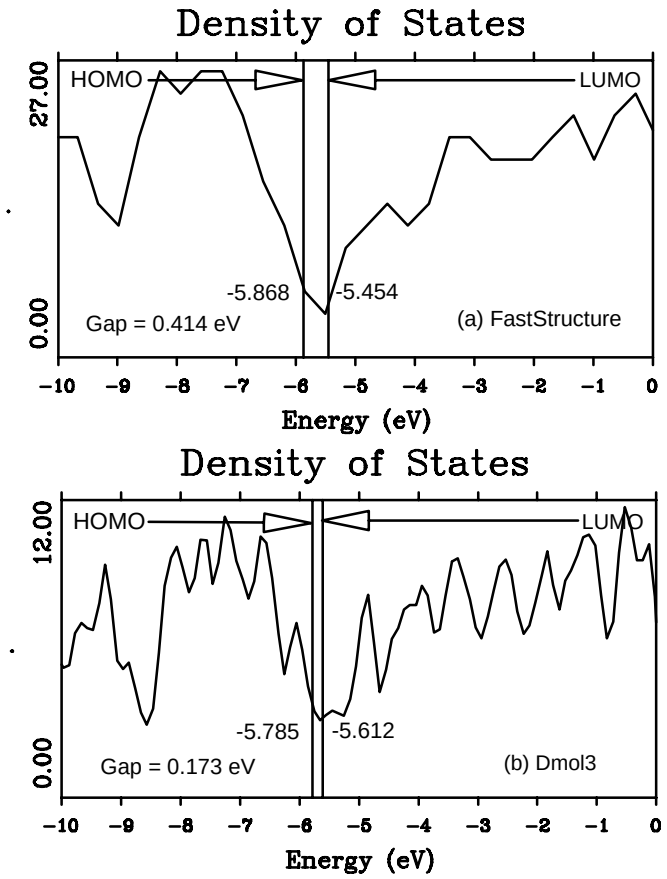
Density of States
HOMO
LUMO
27.00
0.00
-5.868
-5.454
Gap = 0.414 eV
(a) FastStructure
−10 −9 −8 −7 −6 −5 −4 −3 −2 −1 0
Energy (eV)
Density of States
HOMO
LUMO
12.00
0.00
-5.785
-5.612
Gap = 0.173 eV
(b) Dmol3
−10 −9 −8 −7 −6 −5 −4 −3 −2 −1 0
Energy (eV)

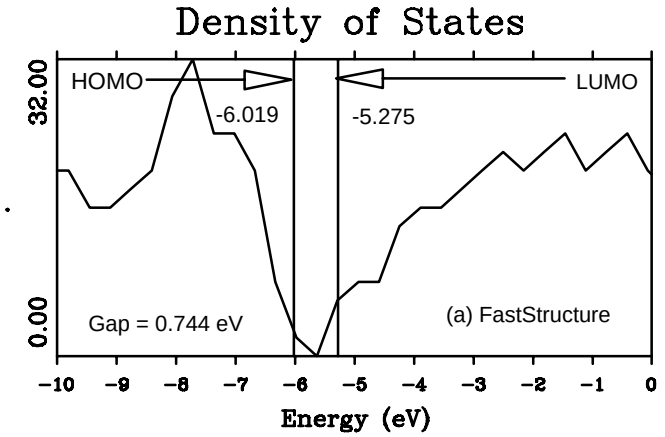
Density of States
HOMO
LUMO
-6.019
-5.275
32.00
0.00
Gap = 0.744 eV
(a) FastStructure
−10 −9 −8 −7 −6 −5 −4 −3 −2 −1 0
Energy (eV)

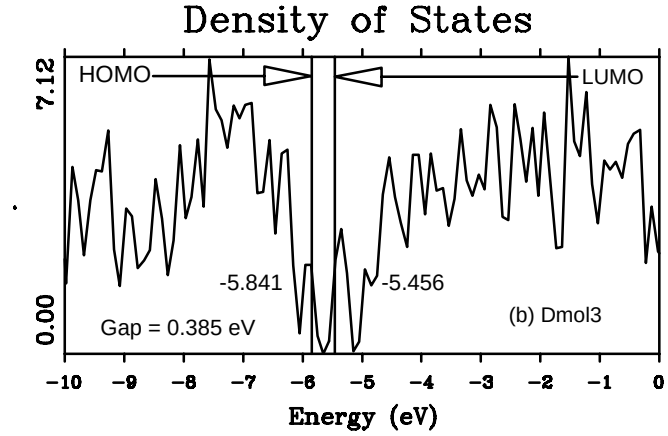
Density of States
HOMO
LUMO
7.12
0.00
-5.841
-5.456
Gap = 0.385 eV
(b) Dmol3
−10 −9 −8 −7 −6 −5 −4 −3 −2 −1 0
Energy (eV)

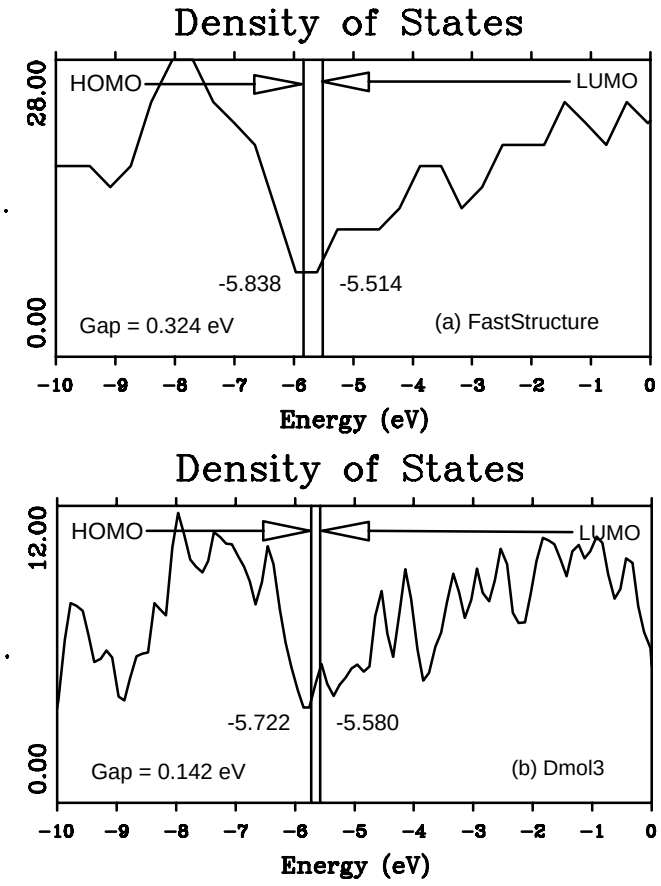
Density of States
28.00
0.00
HOMO
LUMO
-5.838
-5.514
Gap = 0.324 eV
(a) FastStructure
−10 −9 −8 −7 −6 −5 −4 −3 −2 −1 0
Energy (eV)
Density of States
12.00
0.00
HOMO
LUMO
-5.722
-5.580
Gap = 0.142 eV
(b) Dmol3
−10 −9 −8 −7 −6 −5 −4 −3 −2 −1 0
Energy (eV)

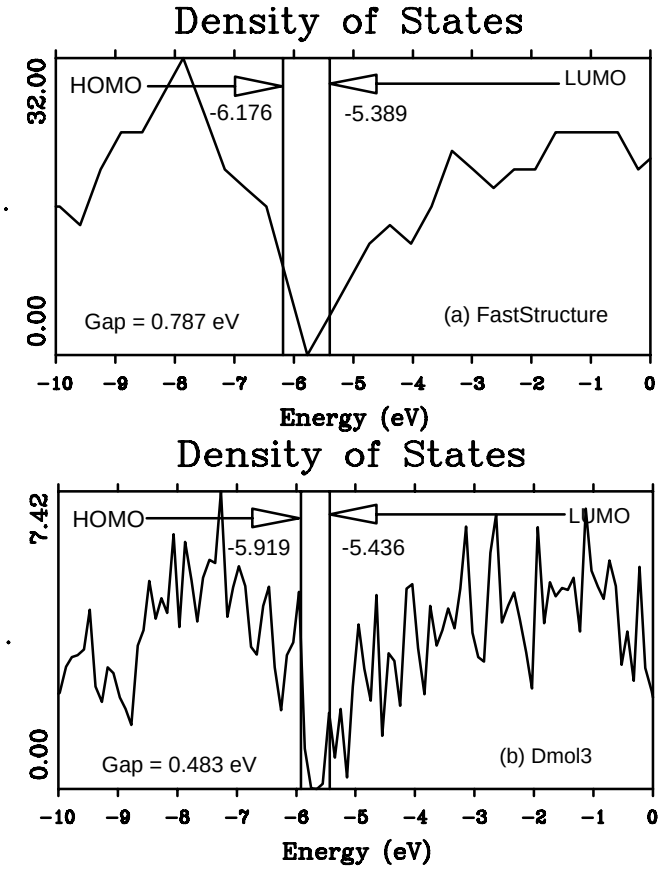
Density of States
32.00
0.00
HOMO
LUMO
-6.176
-5.389
Gap = 0.787 eV
(a) FastStructure
−10 −9 −8 −7 −6 −5 −4 −3 −2 −1 0
Energy (eV)
Density of States
7.42
0.00
HOMO
LUMO
-5.919
-5.436
Gap = 0.483 eV
(b) Dmol3
−10 −9 −8 −7 −6 −5 −4 −3 −2 −1 0
Energy (eV)